Smart Materials and Structures, Volume 30, Issue 3, March 2021, Article number 035013
DOI: 10.1088/1361-665X/abdc05

Micromechanical modeling approach with simplified boundary conditions to compute electromechanical properties of architected piezoelectric composites

Kamran A. Khan[1*], Falah Alhajeri[2], Muhammad Ali Khan[3]

[1]Department of Aerospace Engineering, Khalifa University of Science and Technology, Abu Dhabi, UAE
[2]Department of Mechanical Engineering, Khalifa University of Science and Technology, Abu Dhabi, UAE
[3]School of Aerospace, Transport and Manufacturing, Cranfield University, UK

Abstract

Architected piezoelectric composites (PCs) have recently gained interest in designing transducers and nondestructive testing devices. The current analytical modeling approach cannot be readily applied to design architected periodic PCs exhibiting elastic anisotropy and piezoelectric activity. This study presents a micromechanical (MM)-model based finite element (FE) modeling framework to predict the electromechanical properties (EMPs) of the architected PCs. As an example, the microstructure with one-dimensional (1-3 PCs) connectivity is considered with different cross-section of fibers. 3D FE models are developed. The intrinsic symmetry of architected composite are used to simplify boundary conditions equivalent to periodic boundary conditions (PBCs) . The proposed approach is simple and eliminates the need of a tedious mesh generation process on opposite boundary faces on the MM model of architected PCs. The EMPs of 1-3 PCs calculated from the proposed micromechanics-FE models were compared with those obtained from analytical solutions (i.e. based on micromechanics theories), and FE homogenization (i.e. obtained by employing the PBCs available in the literature). A quite good

* Corresponding author. Tel.: +971-(02) 4018227; Fax: +971-(02) 4472442
E-mail address: kamran.khan@ku.ac.ae (K.A. Khan)

agreement between the proposed modeling approach and the ones obtained using analytical model was observed. However, an excellent agreement is observed with the MM results that employed PBCs. Hence, we have concluded that the proposed MM modeling approach is equivalent to MM models that employed PBCs. The computed enhanced effective elastic, piezoelectric and dielectric properties and corresponding figure of merit (FOM) revealed that 1-3 PCs is suitable in transducer applications.

Keywords: finite element analysis; electromechanical properties, architected piezoelectric composite, unit cell method, piezoelectric materials.

1. Introduction

Piezoelectric ceramics (PCs) are of interest in wide range of transducers applications in smart materials systems and structures [1]. Despite unique EMPs, PCs such as PZT are inherently brittle and are generally dispersed in the form of particle or fiber in polymeric material to create flexible PCs [2] for various industrial applications, such as wearable energy harvesting [3], flexible composite transducer [4], and vibration absorber [5]. Piezoelectric architected composite is the potential subclass of piezoelectric composite in which piezoelectric constituent configuration, such as 1-3 and 3-3, can be optimized to design piezocomposite with required multifunctionality for certain structural applications [6]. Piezocomposite with 1-3 configuration are broadly used in transducer and biomedical devices due to their enhanced coupling coefficient, good acoustic impedance match at interface, and low planar coupling coefficients [1,7]. For various industrial and structural applications there is a need to explore various design of architected piezoelectric composite with tunable EMPs through numerical experimentations and MM homogenization techniques.

PCs are classified according to the connectivity of piezoelectric constituent in different directions, that leads to different electromechanical response [8]. There are numerous experimental studies conducted to understand the affect of connectivity of the constituent on the properties of piezocomposite, such as piezoparticle (0-3 connectivity ([9]); piezofiber (i.e.,1-3 connectivity) ([10]) and cellular piezofiber (i.e.,3-3 connectivity) ([11]). The EMPs of piezocomposite were found to be strongly dependent on fiber architecture and connectivity configuration of the constituents.

Numerous analytical solutions are reported to describe the homogenized behavior of 1-3 PCs. Simplified analytical models are developed using parallel and series connectivity of constituents [12], thin plate approximation for medical ultrasonic transducer [13], and parallel connectivity approach [14]. These models are limited for specific cases and not capable to predict the generalized electromechanical response as they did not provide the complete set of effective electromechanical coefficients. Hashin-Shtrikman approach was proposed to bound the complete set of the effective response of 1-3 type composites [15,16]. However, the range of bounds for some moduli was observed as very wide.

Analytical models based on MM modeling approaches are developed to determine the electromechanical response of 1-3 type PCs with linear electro-mechanical constitutive relations. Most of these micromechanics theories are extension of mechanical homogenization theories [17,18]. For example, Eshelby in his pioneer work introduced Eshelby tensor **S** to relate the macroscopic field variable to microscopic ones, and computed the distribution of stresses, and strains in terms of **S** for an inclusion with ellipsoidal shape in a homogenized infinite-matrix. Later, the expression for Eshelby tensor **S** was determined by Dunn [[19] and Wang [20] for piezocomposite containing elliptical inclusion in a matrix and both constituent following

piezoelectric constitutive law [21]. Based on Eshelby's work, Mori–Tanaka (MT) [22] developed an effective field theory and determined the elastic response of inclusion in an infinite matrix. Dunn and Taya [23] derived an expression for effective electro-elastic moduli of PCs using Mori–Tanaka (MT) method and self-consistent (SC) approach. Levin et al. (2008) developed analytical expression for overall electromechanical response of 1-3 composite using effective field method (EFM). The results agreed with the Mori–Tanaka and Schulgasser's universal relations were satisfied. Nan [24] proposed an effective medium theory (EMT) using multiple-scattering approach (MSA) and Green's function perturbation method to derive explicit relations for overall behavior of PCs.

Most of these micromechanics theories can be used to predict piezoelectric response under various load histories but these theories used average representation of electro-mechanical field with in each phase. Unit cell (UC) models are widely studied, where periodic micro field is applied and the electromechanical field variables are typically solved numerically using FE method [25]. The asymptotic homogenization method (AHM) is adopted by researchers to define the overall response of a periodic piezocomposite containing array of piezofibers with square [26,27] and hexagonal arrangements [28,29]. The complex variable approach and Weierstrass elliptic functions are used to obtain solutions of local problems. Aboudi [30] proposed the method of cells model and Muliana [25] simplified UC model. The piezofibers with square cross-section were homogeneously dispersed in a matrix and the effective electromechanical response of PCs were determined using periodic boundary conditions (PBCs).

Several researchers developed explicit solution and analyzed certain laminated composite geometries like plates, shell, beams and macro fiber composite (MFC) under thermo-electro-mechanical loads and verified with the benchmark results and finite element results. Gohari et al.

[31,32] proposed for the first time a novel explicit exact analytical solution to predict the static deformation, twisting deformation and optimal shape control of smart laminated cantilever composite hybrid plates and beams under arbitrary thermo- electro-mechanical loads using piezoelectric embedded and bounded piezoelectric layers/patches. Results showed that bounded actuator layers/patches found to be a better choice for optimal shape control of smart structures. Gohari et al. [33] proposed an efficient 2D quadratic piezoelectric multilayer shell element by employing first order shear deformation theory to predict the response of laminated composite plate induced by macro fiber composite (MFC) actuators. MFC-d33 type actuators found to be more effective in controlling the large shape deformations. Recently, Tu et al [34] showed that employing third order shear deformation theory (TSDT) can predict the MFC actuation response with higher accuracy. Such analytical solutions would be very useful and effective in validating micromechanical models.

Architected PCs have recently gained interest owing to their unique and tunable mechanical properties and tailorable electromechanical responses. To predict the EMPs of such architected PCs, the microstructural complexity and heterogeneity require to be considered, such as fiber configurations, fiber shape and orientation, and material anisotropy. It is well established that analytical models are useful but their predictive capabilities are limited as these models employed simplified geometries and cannot account for the effect of complex architected microstructure of 0-3, 1-3 and 3-3 type PCs. Finite element analysis is proved to be more suitable. Various MM-models are proposed to compute the overall coefficient of PCs. References [35] [36], [37], [38], [39], [40], [41], [42] and [43], among others used MM models based FE frameworks for computing EMPs of PCs.

Presently, it is not practical to analytically compute the EMPs of architected PCs with 0-3, 1-3, and 3-3 type connectivity. Therefore, the UC homogenization method with PBCs ([35,37,44]) is used to characterize the electromechanical coefficients, understand the role of connectivity, and designing of the piezoelectric composite. The application of PBCs requires UC periodicity and continuity of the field variables (i.e., displacements/electrical potential). This condition requires to mesh all the opposite faces of the FE model in a particular manner such that the difference of the displacements/electric potential can be specified on the corresponding points of all opposite parallel surfaces. In this work, the symmetry of the periodic microstructure is recognized and an explicit mixed traction-displacement boundary conditions (BCs) for UCs is proposed. The continuity of electric electrical charge and displacement field to obtain the overall electromechanical response of architected periodic PCs are incorporated. The proposed approach is simple as there is no need to create a similar mesh on opposite faces of the UC, which requires special consideration by adding extra complexity in the modeling procedure.

This study presents a MM-FE based homogenization approach to determine the EMPs of architected periodic PCs. As an example, the proposed approach is applied to 1-3 piezocomposite. 3D UC models with square array of circular and square fibers are develop. Proposed set of BCs are applied to FE models to calculate the EMPs of 1-3 piezocomposite. The results are compared with different analytical and numerical models, and validated with experimental data.

2. Microstructure of Architected Piezoelectric Composite

We considered unidirectional periodic piezoelectric fiber composites (1-3 piezocomposite) consisting of continuous aligned piezofibers surrounded by a non-piezoelectric isotropic polymeric matrix. In several transducer application, the 1-3 PCs with enhanced performance have recently

found interest. We assumed that the fibers are poled along the 3-direction of the composite. The fiber follows transversely-isotropic piezoelectric constitutive behavior with 6-mm hexagonal symmetry. Most of the 1-3 piezocomposite are manufactured using PZT diced pillars and rods embedded in polymer matrix. Therefore, we considered UC with circular and square cross section fiber surrounded by a polymer. Figure 1 shows the UC of each architecture along with the represented piezocomposite structure.

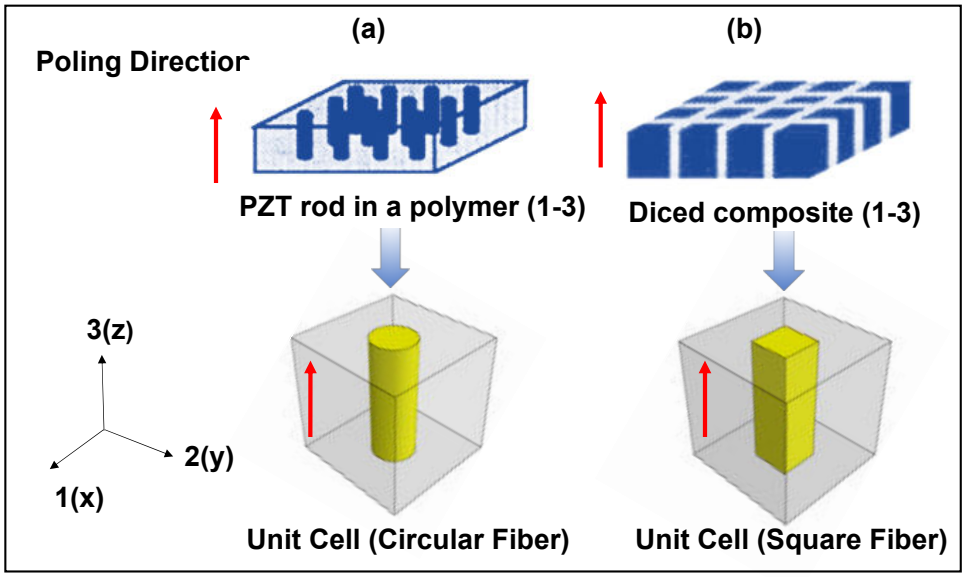

Figure 1. 1-3 periodic piezoelectric composite made of aligned fiber with a) circular-cross section b) square cross-section.

3. Constitutive Model of Piezoelectric Material and Architected Foam

We consider linearized constitutive relations for monolithic piezoelectric materials. The compacted matrix strain-charge form an be expressed as follows:

$$\begin{Bmatrix}\{\varepsilon\}\\ \{D\}\end{Bmatrix} = \begin{bmatrix}[S]^E & [d]\\ [d]^T & [\boldsymbol{\kappa}]^\sigma\end{bmatrix}\begin{Bmatrix}\{\sigma\}\\ \{E\}\end{Bmatrix} \tag{1}$$

Where $\{\varepsilon\}$ and $\{\sigma\}$ represents the strain and stress tensor, and $\{D\}$ and $\{E\}$ are electric displacement, and electric field vectors. Using Voight notation, field variable can be written as

$\sigma = \{\sigma_1, \sigma_2, \sigma_3, \sigma_4, \sigma_5, \sigma_6\}^T$, $\varepsilon = \{\varepsilon_1, \varepsilon_2, \varepsilon_3, \varepsilon_4, \varepsilon, \varepsilon_6\}^T$, D= $\{D_1, D_2, D_3\}^T$, and $E = \{E, E_2, E_3\}^T$. The superscript 'T' denotes the transpose. The matrices $[S^E]$, $[\kappa^\sigma]$, and $[d]$ denotes the compliance tensor, dielectric permittivity tensor and the piezoelectric strain tensor, respectively. The superscript 'E' and 'σ' denote that properties measured at constant E and constant σ, respectively. The third order piezoelectric tensor $[d]$ and fourth order compliance tensor $[S^E]$ can be reduced in matrix form as $d_{ikl} = d_{ib}$ and $S_{ijkl} = S_{ab}$, respectively [45].

The effective properties of the architected PCs can be obtained by taking the average of the field variables over volume. The effective linearized relation in compacted matrix form are expressed as follows:

$$\begin{Bmatrix} \{\bar{\varepsilon}\} \\ \{\bar{D}\} \end{Bmatrix} = \begin{bmatrix} [\bar{S}]^E & [\bar{d}] \\ [\bar{d}]^T & [\bar{\boldsymbol{\kappa}}]^\sigma \end{bmatrix} \begin{Bmatrix} \{\bar{\sigma}\} \\ \{\bar{E}\} \end{Bmatrix} \tag{2}$$

where, $\{\bar{\varepsilon}\}, \{\bar{\sigma}\}, \{\bar{D}\}$, and $\{\bar{E}\}$ are the effective strains, stresses, electric displacement, and electric field. In general, the effective EMPs of architected PCs requires computing 45 independent coefficients, i.e., 21 effective elastic compliance, 18 effective piezoelectric and 6 effective dielectric constants.

In this study we assumed fiber to follow transversely isotropic linearized piezoelectric constitutive behavior which requires 11 independent electromechanical material constants. The constitutive relation in expanded matrix strain-charge form can be expressed as:

$$\begin{Bmatrix} \varepsilon_1 \\ \varepsilon_2 \\ \varepsilon_3 \\ \varepsilon_4 \\ \varepsilon_5 \\ \varepsilon_6 \\ D_1 \\ D_2 \\ D_3 \end{Bmatrix} = \begin{bmatrix} S^E{}_{11} & S^E{}_{12} & S^E{}_{13} & 0 & 0 & 0 & 0 & 0 & -d_{31} \\ S^E{}_{12} & S^E{}_{22} & S^E{}_{23} & 0 & 0 & 0 & 0 & 0 & -d_{32} \\ S^E{}_{13} & S^E{}_{23} & S^E{}_{33} & 0 & 0 & 0 & 0 & 0 & -d_{33} \\ 0 & 0 & 0 & S^E{}_{44} & 0 & 0 & 0 & -d_{24} & 0 \\ 0 & 0 & 0 & 0 & S^E{}_{55} & 0 & -d_{15} & 0 & 0 \\ 0 & 0 & 0 & 0 & 0 & S^E{}_{66} & 0 & 0 & 0 \\ 0 & 0 & 0 & 0 & d_{15} & 0 & \boldsymbol{\kappa}^\sigma{}_{11} & 0 & 0 \\ 0 & 0 & 0 & d_{24} & 0 & 0 & 0 & \boldsymbol{\kappa}^\sigma{}_{22} & 0 \\ d_{31} & d_{32} & d_{33} & 0 & 0 & 0 & 0 & 0 & \boldsymbol{\kappa}^\sigma{}_{33} \end{bmatrix} \begin{Bmatrix} \sigma_1 \\ \sigma_2 \\ \sigma_3 \\ \sigma_4 \\ \sigma_5 \\ \sigma_6 \\ E_1 \\ E_2 \\ E_3 \end{Bmatrix} \quad (3)$$

For transversely isotropic piezoelectric aligned fibers (PZT) arranged in a square array and surrounded by an isotropic material, the effective response of such composite can still be represented by transversely-isotropic piezosolid with tetragonal (crystal class 4mm) symmetry and we need to compute the 11 independent effective material constants including 6 elastic moduli, 3 piezoelectric constants and 2 dielectric coefficients, respectively. The constitutive relations for homogenized piezocomposite are expressed in expanded matrix stress-charge form as follows:

$$\begin{Bmatrix} \sigma_1 \\ \sigma_2 \\ \sigma_3 \\ \sigma_4 \\ \sigma_5 \\ \sigma_6 \\ D_1 \\ D_2 \\ D_3 \end{Bmatrix} = \begin{bmatrix} C^E{}_{11} & C^E{}_{12} & C^E{}_{13} & 0 & 0 & 0 & 0 & 0 & -e_{31} \\ C^E{}_{12} & C^E{}_{11} & C^E{}_{13} & 0 & 0 & 0 & 0 & 0 & -e_{31} \\ C^E{}_{13} & C^E{}_{13} & C^E{}_{33} & 0 & 0 & 0 & 0 & 0 & -e_{33} \\ 0 & 0 & 0 & C^E{}_{44} & 0 & 0 & 0 & -e_{15} & 0 \\ 0 & 0 & 0 & 0 & C^E{}_{44} & 0 & -e_{15} & 0 & 0 \\ 0 & 0 & 0 & 0 & 0 & C^E{}_{66} & 0 & 0 & 0 \\ 0 & 0 & 0 & 0 & e_{15} & 0 & \boldsymbol{\kappa}^\sigma{}_{11} & 0 & 0 \\ 0 & 0 & 0 & e_{15} & 0 & 0 & 0 & \boldsymbol{\kappa}^\sigma{}_{11} & 0 \\ e_{31} & e_{31} & e_{33} & 0 & 0 & 0 & 0 & 0 & \boldsymbol{\kappa}^\sigma{}_{33} \end{bmatrix} \begin{Bmatrix} \varepsilon_1 \\ \varepsilon_2 \\ \varepsilon_3 \\ \varepsilon_4 \\ \varepsilon_5 \\ \varepsilon_6 \\ E_1 \\ E_2 \\ E_3 \end{Bmatrix} \quad (4)$$

4. Micromechanical Finite Element Analysis of Architected Piezoelectric Composites

In this study, we have extended our previously developed MM-FE homogenization framework **[46]** for periodic architected elastic solids to periodic architected PCs. A mixed BCs equivalent to

PBCs are established and applied on a UC to calculate the effective EMPs of architected PCs using the constituent properties and connectivity configuration of the constituents in the UC.

FE models of 1-3 type PCs are generated by varying the volume fraction (V_f) values of aligned piezoelectric fibers ranging from 0-70% were embedded in a polymer matrix material. For 1-3 PCs with PZT rods, a UC with circular cross section fiber was generated while a UC with square cross section fiber was developed to represent 1-3 piezocomposite with PZT diced pillars. Figures 2 (a) and (b) show a representative UC of 1-3 PCs. Figure 2 also shows the example of the UC. The axes direction on 6 boundary faces are also shown.

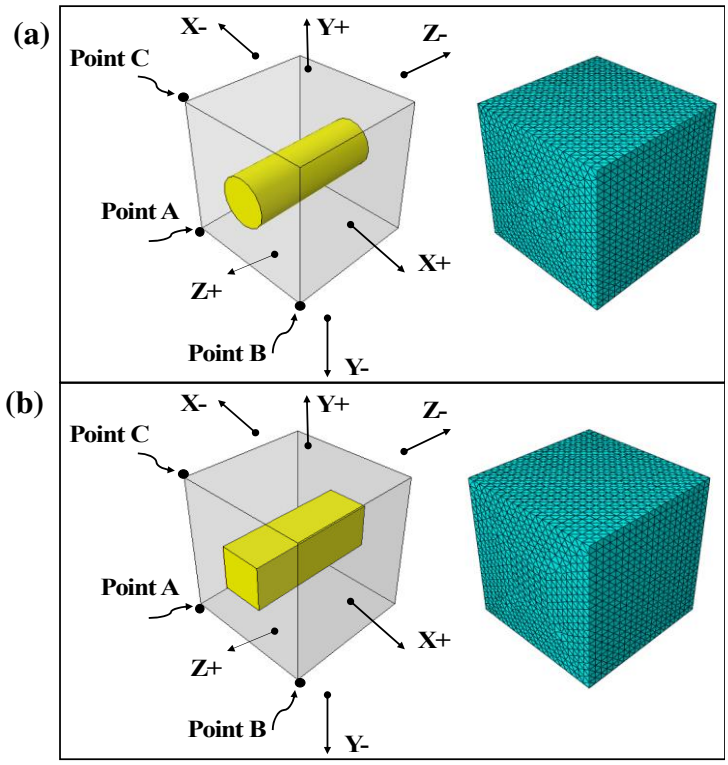

Figure 2. Example of a geometrical UC model and FE model meshed with C3D10E elements. (a) circular fiber, (b) square fiber

All the FE analysis were performed using ABAQUS© and every material point in the UC of PCs is assumed to be poled along z-axis. The electric polarization is related to the electric displacement through $\boldsymbol{P} = \boldsymbol{D} - \kappa_0 \boldsymbol{E}$, where $\kappa_0 = 8.85\text{x}10^{-12}$ F/m is the permittivity of the free space. The C3D10E element was used to mesh the UC, which has 3 displacements (u) DOF and 1 for electrical potential (ϕ). When electrical loading is applied to UC then the rigid body motion should be avoided by constraining points A, B, and C appropriately, as shown in Figure 2.

PBCs are classically imposed on UC to determine the homogenized properties of infinite periodic microstructures ([47], [48], [49]). PBCs yield acceptable respoonse as compared to other homogeneous type BCs ([50], [51]). Ensuring the continuity of u's and the ϕ and periodicity of UC, Xia et al. [51] derived PBCs for u, i.e., $u_m^{n+}(x,y,z) - u_m^{n-}(x,y,z) = \Gamma_m^n, (m,n = 1,2,3)$. Where Γ_m^n with $(m,n = 1,2,3)$ denote deformations along longitudinal directions and Γ_m^n with $(m \neq n)$ represent shear deformations. The position and negative x_j direction faces are represented by $n^+$and n^-, respectively. The PBCs for ϕ can be written by $\phi_m^{n+}(x,y,z) - \phi_m^{n-}(x,y,z) = \overline{E_m}(\, x_m^{n+} - x_m^{n-})$, with $(m = n = 1,2,3)$, where $\bar{E}_i$ denote the applied effective E. The periodicity requirement of displacement on two opposite faces sometime needs a tedious mesh generation process, when architected periodic microstructures is complex.

For periodic microstructures, Li [52] derived MBCs which were equivalent to PBCs to compute their elastic response. Recently, Khan and Khan [53] extended Li's [52] effort and incorporated continuity of ϕ to derive the mixed BCs and obtained effective EMPs of architected periodic PCs, as shown in Figure 3.

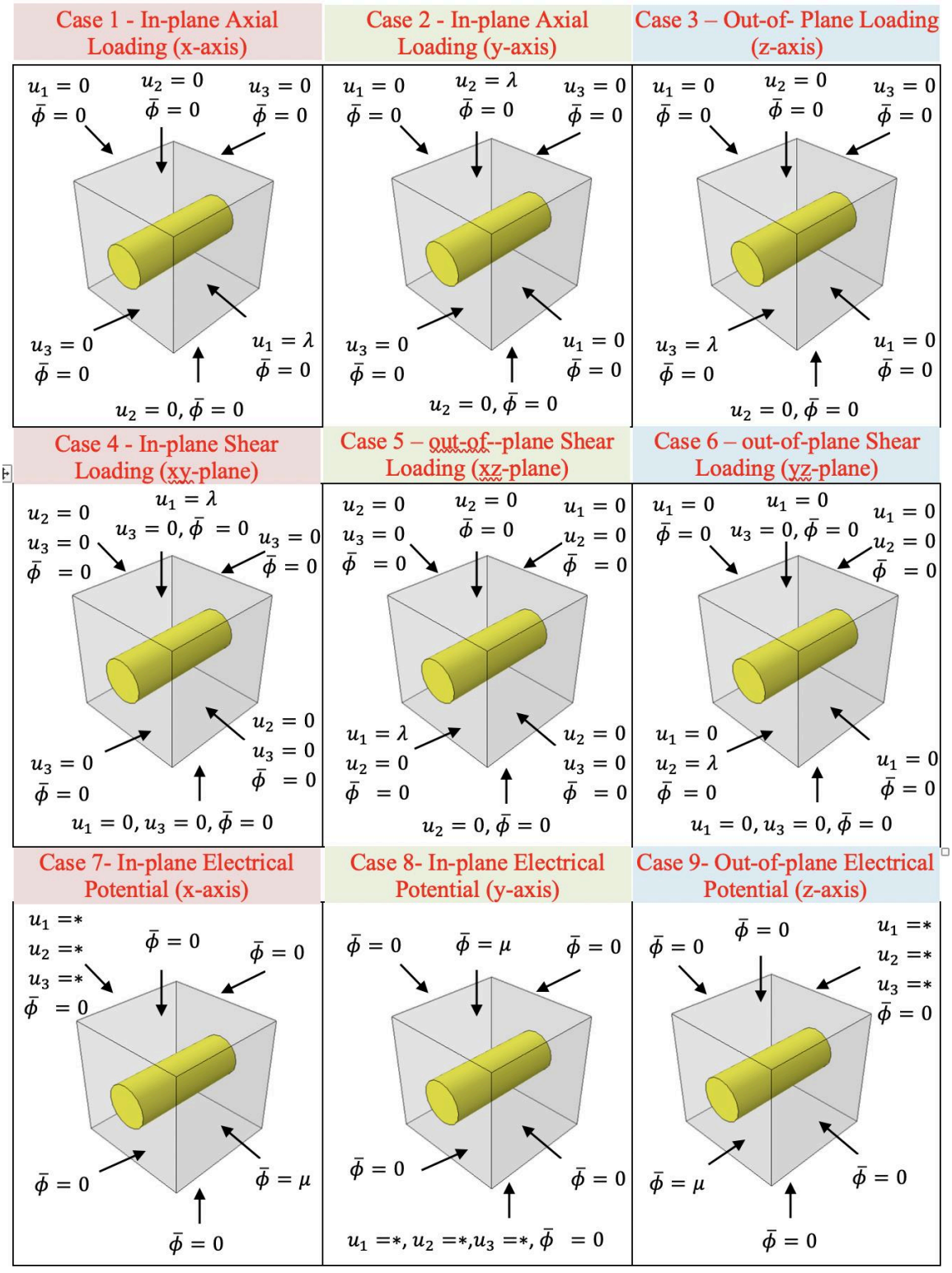

Fig. 3. Adapted mixed boundary conditions to compute the EMPs of PCs.

5. Analytical Models

Next, we will briefly discuss the analytical models which are used in this present study for comparison. We will present the results of those analytical models which supposed that the aligned fibers are uniformly distributed in the polymer matrix with square array packing or randomly distribute to represent the homogenized response equivalent to statistically homogeneous medium. The linear piezoelectric behavior was assumed for the constituents.

5.1 Mori-Tanaka Model (Effective Field Theory)

The MM modeling approach was used by Dunn and Taya [23] to establish the relation of effective EMPs of a two-phase PCs as a function of V_f and typical microstructures of piezoelectric fiber including continuous cylinder, ribbon-like, and ellipsoidal. Here, we briefly describe the approach adopted by Dunn and Taya [23] to describe the electromechanical behavior of PCs. The piezoelectric materials constitutive relations described in Eq (1) can be represented as

$$\Sigma_{iP} = E_{iPQn} Z_{Qn} \tag{7}$$

Where $Z_{Qn}, \Sigma_{iP},$ and E_{iPQn} are not tensors and E_{iPQn} represents the electro-elastic moduli matrix. where lowercase subscript ranges 1,2,3 while upper case subscript ranges 1,2,3,4. In terms of the field variables discussed in Eq (1),

$$Z_{Mn} = \begin{cases} \varepsilon_{mn}, & (Q = 1,2,3) \\ -\phi_{,n}, & (Q = 4) \end{cases} \tag{8}$$

$$\Sigma_{iJ} = \begin{cases} \sigma_{ij}, & (P = 1,2,3) \\ D_i, & (P = 4) \end{cases} \tag{9}$$

$$\mathrm{E}_{iJMn} = \begin{cases} C_{ijmn}, & (P, Q = 1,2,3) \\ e_{nij}, & (P = 1,2,3;\ Q = 4) \\ \sigma_{imn}, & (P = 4; Q = 1,2,3) \\ \kappa_{in}, & (P, Q = 4) \end{cases} \tag{10}$$

where σ_{ij}, ε_{ij}, $\phi_{,i}, D_i$ are the stress tensor, strain tensor, electric potential gradient and displacement vector. The effective behavior of PCs is related by averaging the field quantities over the volume (σ_{ij}, ε_{ij}, D_i, and $\phi_{,i}$)

$$\bar{\boldsymbol{\Sigma}} = \boldsymbol{E}\,\bar{\mathbf{Z}} \tag{11}$$

$$\bar{\boldsymbol{\Sigma}} = (1-c)\bar{\boldsymbol{\Sigma}}_{\mathbf{1}} + \boldsymbol{c}\bar{\boldsymbol{\Sigma}}_{\mathbf{2}} \tag{12}$$

$$\bar{\mathbf{Z}} = (1-c)\bar{\mathbf{Z}}_{\mathbf{1}} + \boldsymbol{c}\bar{\mathbf{Z}}_{\mathbf{2}} \tag{13}$$

The bold letter represent vector 9 x 1 or matrix 9 x 9 and the overbar represents the average quantity over volume. The c denotes the V_f of the piezoelectric fiber and subscript 1 represent matrix and 2 denote the piezoelectric inclusion. Using the constitutive relation of each constituent and Eq. (8)-(10), the effective electro-elastic moduli is written as

$$\mathbf{E} = \mathbf{E}_{\mathbf{1}} + c(\mathbf{E}_{\mathbf{2}} - \mathbf{E}_{\mathbf{1}})\boldsymbol{A} \tag{14}$$

The average ε_{ij} and $\phi_{,i}$ in piezoelectric fiber is related to macroscopic field variables through the strain-potential gradient concentration matrix **A**. According to Mori-Tanaka [22] effective field theory **A** can be expressed as

$$\mathbf{A} = \mathbf{A}^{\boldsymbol{dil}}\left[(1-c)\,\boldsymbol{I} + c\,\mathbf{A}^{\boldsymbol{dil}}\right]^{-\mathbf{1}} \textbf{ with } \mathbf{A}^{\boldsymbol{dil}} = \left[\boldsymbol{I} + \boldsymbol{S}\,\boldsymbol{E}_{\mathbf{1}}^{-\mathbf{1}}\,(\mathbf{E}_{\mathbf{2}} - \mathbf{E}_{\mathbf{1}})\right]^{-\mathbf{1}} \tag{15}$$

The expression of effective electro-elastic moduli depends on E_1, E_2, c and shape of the architecture shape through the constraint tensor S. The S is the coupled electro-elastic Eshelby's tensor and its components are determined explicitly for 1-3 type connectivity is obtained by Dunn and Taya [54]. For 1-3 piezocomposite, the non-zero components of S are as follows:

$$S_{1111} = S_{2222} = (5C_{11} + C_{12})/(8C_{11}) \tag{16}$$

$$S_{1212} = S_{2121} = S_{1221} = S_{2112} = (3C_{11} - C_{12})/(8C_{11}) \tag{17}$$

$$S_{1313} = S_{3131} = S_{1331} = S_{3113} = S_{2323} = S_{3232} = S_{2332} = S_{3223} = 0.5 \tag{18}$$

$$S_{1122} = S_{2211} = (3C_{12} - C_{11})/(8C_{11}) \tag{19}$$

$$S_{1133} = S_{2233} = (C_{13})/(2C_{11}) \quad (20)$$

$$S_{1143} = S_{2243} = (e_{31})/(2C_{11}) \quad (21)$$

$$S_{4141} = S_{4242} = 1/2 \quad (22)$$

5.2 Effective Field Method (EFM)

Now, we briefly describe the EFM used by Levin et al. [55] to derive the explicit close form equations for the effective EMPs. The linear piezoelectric material is defined as $J = \boldsymbol{L}F$ with $J = [\sigma, D]$**,** $F = [\kappa, E]$, and L is the linear operator representing the electroelastic constants matrix. This approach considered a piezocomposite consists of aligned cylindrical fiber with electro-elastic characteristics operator $L = L_0 + L_1$ surrounded by a matrix with an electro-elastic characteristic operator L_0. The effective response can be expressed as $\langle J \rangle = \boldsymbol{L}^* \langle F \rangle$, where $\langle \quad \rangle$ represent the average fields and $\boldsymbol{L}^*$ is the electro-elastic characteristic operator of the PCs, $\boldsymbol{L}^* = \boldsymbol{L^0} + \boldsymbol{n_0 Q}$**.** Here $\boldsymbol{n_0}$ is the fiber concentration and $\boldsymbol{Q}$ is an operator that need to be constructed by solving the electrostatic-problem for a single fiber surrounded by a homogeneous medium. Levin et al. [55] constructed the operator Q by solving an isolated fiber problem while accounting for the presence of the surrounding fiber using the effective field method and obtained explicit expression of overall EMPs of PCs. Some of the relevant constants are shown below

$$\frac{1}{2}(C_{11} + C_{12}) = \frac{1}{2}(C_{11}^m + C_{12}^m) + \frac{1}{2}c(C_{11}^f + C_{12}^f)\left[1 + (1-c)(C_{11}^f + C_{12}^f)/2C_{11}^m\right]^{-1} \quad (23)$$

$$C_{13} = C_{13}^m + c\, C_{13}^f\left[1 + (1-c)(C_{11}^f + C_{12}^f)/2C_{11}^m\right]^{-1} \quad (24)$$

$$C_{33} = C_{33}^m + c\left\{C_{33}^f - (1-c)\left(C_{13}^f\right)^2/C_{11}^m\left[1 + (1-c)(C_{11}^f + C_{12}^f)/2C_{11}^m\right]^{-1}\right\} \quad (25)$$

$$C_{66} = \frac{1}{2}(C_{11} - C_{12}) = C_{66}^m + c\, C_{66}^f\left[1 + (1-c)C_{66}^f(1/C_{11}^m + 1/C_{66}^m)/2\right]^{-1} \quad (26)$$

$$e_{31} = e_{31}^m + c\, e_{31}^f\left[1 + (1-c)(C_{11}^f + C_{12}^f)/2C_{11}^m\right]^{-1} \quad (27)$$

$$e_{33} = C_{13}^{m} + c\left\{e_{33}^{f} - (1-c)(C_{13}^{f}e_{33}^{f})/C_{11}^{m}\left[1 + (1-c)(C_{11}^{f} + C_{12}^{f})/2C_{11}^{m}\right]^{-1}\right\} \quad (28)$$

$$\kappa_{33} = \kappa_{33}^{m} + c\left\{\kappa_{33}^{f} + (1-c)\left(e_{31}^{f}\right)^{2}/C_{11}^{m}\left[1 + (1-c)(C_{11}^{f} + C_{12}^{f})/2C_{11}^{m}\right]^{-1}\right\} \quad (29)$$

Details expression of other effective electromechanical constants of piezoelectric constants can be found in the referred article [55]. Interestingly, the EFM results of electromechanical constants exactly match with the coefficients determined using Mori-Tanaka method [22].

5.3 Asymptotic Homogenization Method

Guinovart-D´ıaz et al. (2001) presented the analytical expression of the effective EMPs of piezoelectric fiber reinforced composite with periodic distributed unidirectional fibers in square array packing. The linear constitutive equations with quickly fluctuating coefficients are turned to effective electroelastic constants ($\bar{\mathbf{C}}^{\boldsymbol{E}}, \bar{\mathbf{e}}, \bar{\boldsymbol{\kappa}}^{\boldsymbol{\varepsilon}}$). To compute the local and average response of composite a complex variable approach was employed. Some of the overall material constants expressions are as follows:

$$C_{13} = C_{23} = (1-c)\,C_{13}^{m} + c\,C_{13}^{f} + c\left(C_{13}^{m} - C_{13}^{f}\right)\left(C_{11}^{m} - C_{11}^{f} + C_{12}^{m} - C_{12}^{f}\right)\alpha_1 / 2C_{66}^{m}$$

$$C_{33} = (1-c)\,C_{33}^{m} + c\,C_{33}^{f} + c\left(C_{13}^{m} - C_{13}^{f}\right)^{2}\alpha_1 / C_{66}^{m}$$

$$C_{66} = (1-c)\,C_{66}^{m} + c\,C_{66}^{f} - c\left(C_{66}^{m} - C_{66}^{f}\right)\alpha_3$$

$$e_{31} = (1-c)\,e_{31}^{m} + c\,e_{31}^{f} + c\left(e_{31}^{m} - e_{31}^{f}\right)\left(C_{11}^{m} - C_{11}^{f} + C_{12}^{m} - C_{12}^{f}\right)\alpha_1 / 2C_{66}^{m}$$

$$e_{33} = (1-c)\,e_{33}^{m} + c\,e_{33}^{f} + c\left(C_{13}^{m} - C_{13}^{f}\right)\left(e_{31}^{m} - e_{31}^{f}\right)\alpha_1 / C_{66}^{m}$$

$$\kappa_{33} = (1-c)\,\kappa_{33}^{m} + c\,\kappa_{33}^{f} - c\left(e_{31}^{m} - e_{31}^{f}\right)^{2}\alpha_1 / C_{66}^{m}$$

Where α_1 and α_3 are parameters that depends on the fiber arrangement, electromechanical constants of each constituents and V_f of piezoelectric fiber. The superscript m and f denote matrix and fiber, respectively. Details expression of these parameters and other effective electromechanical constants of piezoelectric constants can be found in the referred article [56].

6. Results

The proposed set of BCs were applied to the UC and the electromechanical coefficients of the PCs were computed for each load case given in Figure 2. The BCs were applied such that for each load case there is only one non-zero component of effective stress and electric field vector remains on the right side of the Equation (2). For each load case, the computation of some of the typical electromechanical coefficients are also shown in Table 1. In general, the application of complete set of BCs on UC and employing Equation (2) can yield up to 45 independent coefficients. For this study, we assumed that the transversely isotropic piezoelectric aligned fibers (PZT) are arranged in a square array and surrounded by an isotropic matrix, the effective response of such composite can still be represented by transversely-isotropic piezosolid with tetragonal (crystal class 4mm) symmetry and we need to compute the 11 independent material parameters.

The FE computation will compute effective elastic compliance, $\bar{S}^{E}_{ijkl}$, piezoelectric strain tensors, $(\bar{d}^{E}_{kij}, \bar{d}^{\sigma}_{ikl})$, dielectric stress tensor $\bar{\kappa}^{\sigma}_{ij}$. Several other material parameters are also needed to characterized the behavior of piezoelectric materials, such as, other elastic properties $\bar{C}^{E}_{ijkl}$, $\left[\boldsymbol{C}^{D}\right]$, and $\left[\boldsymbol{S}^{D}\right]$, piezoelectric stress tensor $\left[\boldsymbol{e}\right]$, dielectric strain tensor $\left[\kappa^{\varepsilon}\right]$, piezoelectric voltage $\left[\boldsymbol{g}\right]$, and current constants $\left[\boldsymbol{h}\right]$, respectively. These constants can be found using relations given in reference [45].

Table 1. Complete set of boundary conditions with computation formulae to determine electromechanical coefficients.

Load Case	Coefficients	X^-	X^+	Y^-	Y^+	Z^-	Z^+	Relation

		$\bar{u}_i/\,\bar{\phi}$	$\bar{u}_i/\,\bar{\phi}$	$\bar{u}_i/\,\bar{\phi}$	$\bar{u}_i/\,\bar{\phi}$	$\bar{u}_i/\,\bar{\phi}$	$\bar{u}_i/\,\bar{\phi}$	
1	$\bar{S}^E_{11}, \bar{S}^E_{12}$ $\bar{S}^E_{13}, \bar{d}^E_{31}$	$0\,/\,0$	$\overline{u_1}/\,0$	$0\,/\,0$	$-/\,0$	$0\,/\,0$	$-/\,0$	$\bar{\varepsilon}_1/\bar{\sigma}_1, \bar{\varepsilon}_2/\bar{\sigma}_1$ $\bar{\varepsilon}_3/\bar{\sigma}_1, \bar{D}_3/\bar{\sigma}_1$
2	$\bar{S}^E_{21}, \bar{S}^E_{22}$ $\bar{S}^E_{23}, \bar{d}^E_{32}$	$0\,/\,0$	$-/\,0$	$0\,/\,0$	$\overline{u_2}/\,0$	$0\,/\,0$	$-/\,0$	$\bar{\varepsilon}_1/\bar{\sigma}_2, \bar{\varepsilon}_2/\bar{\sigma}_2$ $\bar{\varepsilon}_3/\bar{\sigma}_2, \bar{D}_3/\bar{\sigma}_2$
3	$\bar{S}^E_{31}, \bar{S}^E_{32}$ $\bar{S}^E_{33}, \bar{d}^E_{33}$	$0\,/\,0$	$-/\,0$	$0\,/\,0$	$-/\,0$	$0\,/\,0$	$\overline{u_3}/\,0$	$\bar{\varepsilon}_1/\bar{\sigma}_3, \bar{\varepsilon}_2/\bar{\sigma}_3$ $\bar{\varepsilon}_3/\bar{\sigma}_3, \bar{D}_3/$ $\bar{\sigma}_3$
4	$\bar{S}^E_{44}, \bar{d}^E_{24}$	$\overline{u_2}=0$ $\overline{u_3}=0$ $/0$	$\overline{u_2}=0$ $\overline{u_3}=0$ $/0$	$\overline{u_1}=0$ $\overline{u_3}=0$ $/0$	$\overline{u_1}\neq 0$ $\overline{u_3}=0$ $/0$	$\overline{u_3}=0$ $/0$	$\overline{u_3}=0$ $/0$	$\bar{\varepsilon}_4/\bar{\sigma}_4,$ $\bar{D}_2/\bar{\sigma}_4$
5	$\bar{S}^E_{55}, \bar{d}^E_{15}$	$\overline{u_2}=0$ $\overline{u_3}=0$ $/0$	$\overline{u_2}=0$ $\overline{u_3}=0$ $/0$	$\overline{u_2}=0$ $/0$	$\overline{u_2}=0$ $/0$	$\overline{u_1}=0$ $\overline{u_2}=0$ $/0$	$\overline{u_1}\neq 0$ $\overline{u_2}=0$ $/0$	$\bar{\varepsilon}_5/\bar{\sigma}_5,$ $\bar{D}_1/\bar{\sigma}_5$
6	$\bar{S}^E_{66}$	$\overline{u_1}=0$ $/0$	$\overline{u_1}=0$ $/0$	$\overline{u_1}=0$ $\overline{u_3}=0$ $/0$	$\overline{u_1}=0$ $\overline{u_3}=0$ $/0$	$\overline{u_1}=0$ $\overline{u_2}=0$ $/0$	$\overline{u_1}=0$ $\overline{u_2}\neq 0$ $/0$	$\bar{\varepsilon}_6/\bar{\sigma}_6$
7	$\bar{d}^\sigma_{15}, \bar{\kappa}^\sigma_{11}$	$*/\,0$	$-/\,\bar{\phi}$	$-/-$	$-/-$	$-/-$	$-/-$	$\bar{\varepsilon}_5/\bar{E}_1,$ $\bar{D}_1/\bar{E}_1$
8	$\bar{d}^\sigma_{24}, \bar{\kappa}^\sigma_{22}$	$-/-$	$-/-$	$*/\,0$	$-/\,\bar{\phi}$	$-/-$	$-/-$	$\bar{\varepsilon}_4/\bar{E}_2,$ $\bar{D}_2/\bar{E}_2$
9	$\bar{d}^\sigma_{31}, \bar{d}^\sigma_{32}$ $\bar{d}^\sigma_{33}, \bar{\kappa}^\sigma_{33}$	$-/-$	$-/-$	$-/-$	$-/-$	$*/\,0$	$-/\,\bar{\phi}$	$\bar{\varepsilon}_1/\bar{E}_3, \bar{\varepsilon}_2/\bar{E}_3$ $\bar{\varepsilon}_3/\bar{E}_3, \bar{D}_3/\bar{E}_3$

*Points A, B and C are constrained on respective faces (having zero electric potential) to avoid rigid body motion.

6.1 Comparison with the numerical and analytical models

The validity and limitations of proposed MM model is further shown by comparing the results with those obtained from experimental data, other MM models with PBCs by Berger et al. [37] referred as Numerical-PBC, Lin and Muliana [25] referred as UC-Square Fiber and analytical models by Dunn and Taya [23] referred as MT, Asymptotic homogenization method by Diaz et al. [56] referred as AHM, Effective field method by Levin et al. [55] referred as EFM. The material parameters of ceramic fiber and polymer used in the computation were obtained from [35] and are given in table 2. The permittivity of free space is $\kappa_0 = 8.85 \times 10^{-12}$.

Table 2. Properties of the PZT-7A piezofiber and the Araldite D Epoxy.

Properties	PZT-7A	Araldite D
$C_{11}^E = C_{22}^E\ (GPa)$	154.84	8.0
$C_{12}^E = C_{21}^E\ (GPa)$	83.237	4.4
$C_{13}^E = C_{31}^E = C_{23}^E = C_{32}^E (GPa)$	82.712	4.4
$C_{33}^E\ (GPa)$	131.39	8.0
$C_{44}^E = C_{55}^E (GPa)$	25.696	1.8
$C_{66}^E\ (GPa)$	35.800	1.8
$e_{15} = e_{24}\ (\mathrm{C}/m^2)$	9.3495	-
$e_{31} = e_{32}\ (\mathrm{C}/m^2)$	-2.1205	-
$e_{33}\ (\mathrm{C}/m^2)$	9.5218	-
$\kappa_{11}^{\varepsilon} = \kappa_{22}^{\varepsilon}$ (n C/Vm)	4.065	0.0372
$\kappa_{33}^{\varepsilon}$ (n C/Vm)	2.079	0.0372
Density, $\rho\ (Kg/m^3)$	7600	1150

First, we have compared the elastic constants with the MM model (employing PBCs) and analytical models. In Figure 4, the elastic constants of the PZT-7A/Araldite D piezocomposite got from the MM models established in the current study with several other analytical models and MM models with PBCs; as a function of fiber V_f. The figures show that the results estimated by the current MM model and those predicted by MM models with PBCs are in excellent agreement over almost the whole range of fiber V_f. However, the theoretical predictions of C_{11} and C_{12} show essentially the same trend but are only indistinguishable at low V_f of fiber. A similar trend is observed in literature using MM model with PBCs [57]. The possible explanation is that the elastic constants show highly nonlinear behavior at higher V_f which is generally not considered in analytical model homogenization formulations. Other reasons of the disagreements are possibly the existence of large difference in the properties of both constituents. For this situation, the inclusion interaction especially at higher inclusion V_f are the main reason for deviations of results of MM model from analytical models. The figure 4 shows that the moduli are anisotropic in nature

and display dissimilar trends. Most of the elastic constants except longitudinal stiffness constant C_{33} shows nonlinear trend with the increase of V_f of fiber.

The results of effective elastic response of composite with square array of circular and square fiber shows that the macroscopic piezocomposite change its symmetry from hexagonal symmetry 6 mm to the tetragonal crystal symmetry of 4-mm.

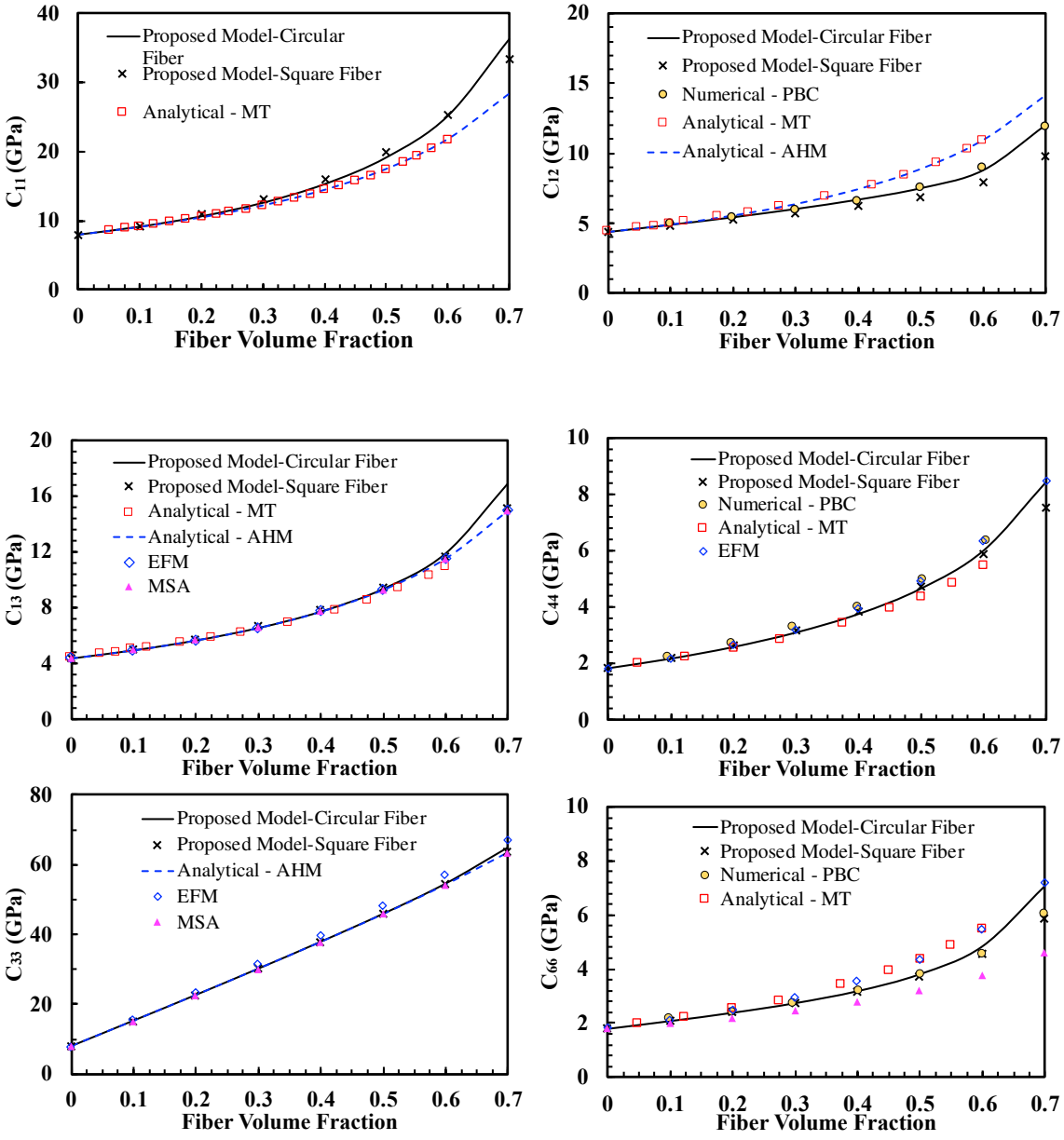

Figure 4. Comparison of elastic constants for PZT-7A/Epoxy piezocomposite obtained from the MM models developed in the current study with several other analytical models and numerical models with PBCs; vs fiber V_f, variations of the (a) C_{11}, (b) C_{12}, (c) C_{13}, (d) C_{44}, (e) C_{33}, (f) C_{66}

Next, the results of electromechanical coupling and dielectric properties are compared with the analytical and numerical models. The variation of the longitudinal- and shear-electromechanical coefficients are plotted against fiber volume-fraction (V_f) in Figure 5. A significant dependence on the V_f of the fiber is observed for both longitudinal and shear coupling piezoelectric properties, as shown in Figure 5 (a) and b). Both piezoelectric constants exhibit almost same dependencies and values increase nonlinearly with the increase of V_f, as shown in Figure 5 (c). In contrast, the normal coupling parameter show linear dependence on the V_f of fiber. For monolithic materials, the longitudinal electromechanical coupling properties along the 3- directions, i.e., e_{33} are often considered the most important parameter to help identifying the utility of the piezoelectric material in particular industrial applications. A quite agreement of the proposed model results with the numerical and analytical models is observed. Figure 5 (d) and (e) show the effective dielectric properties with respect to fiber V_f. The dielectric constants $\kappa_{11}^{\varepsilon}$ exhibit nonlinear dependence on the piezoelectric fiber V_f and can be associated with the increase in electric charges because of the presence of more fiber at higher V_f. In contrast, the longitudinal dielectric constants $\kappa_{33}^{\varepsilon}$ show linear dependence proportional to the fiber area increase along the application of the electric field and poling direction. Excellent agreement with the analytical and numerical model is observed while comparing the ones obtained using the proposed MM model.

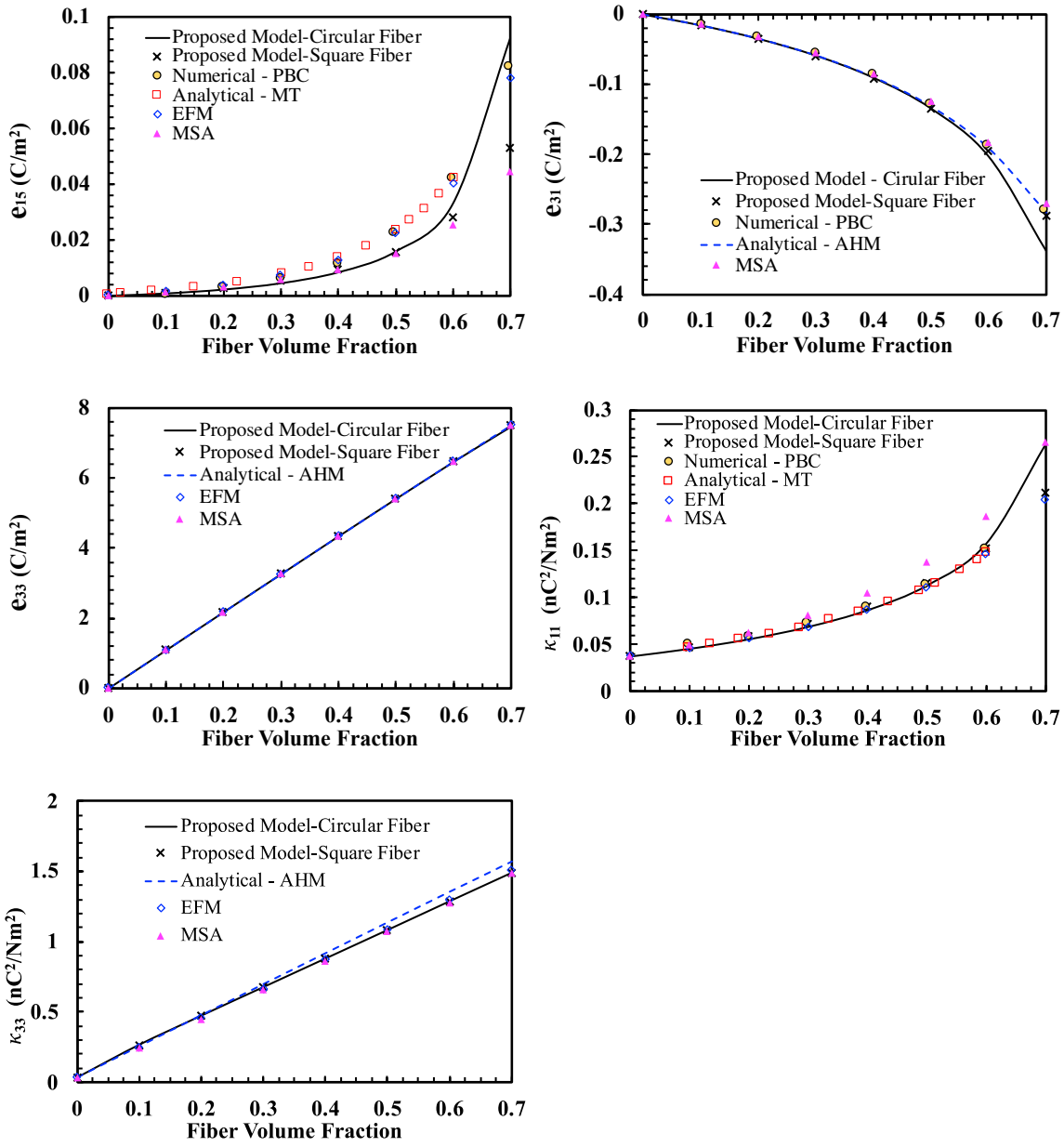

Figure 5. Comparison of material constants for PZT-7A/Epoxy piezocomposite obtained from the MM models proposed in the current work with several other analytical models and numerical models with PBCs; vs fiber V_f, variations of the (a) e_{15}, (b) e_{31}, (c) e_{33}, (d) $\kappa_{11}^{\varepsilon}$, (e) $\kappa_{33}^{\varepsilon}$.

The results of the current work are in decent agreement with the MM model that used PBCs. However, a quite good agreement is observed when compared with the analytical models except some coefficients show slight deviation at higher V_f, such as C_{11}, C_{22}, C_{66}, e_{31}, e_{15}, and κ_{11}. To show more evidence for the validity of the presented model's results, we compared them at 60%

fiber V_f with the effective constants obtained from other MM models that used PBCs, reported by Berger et al. [37] and Pettermann and Suresh [35] and analytical solution of Levin et al. [55] and Hashin/Shtrikman bounds [58]. Moreover, we have compared the predictions by the proposed model with the bounds for piezoelectric composited consist of aligned continuous fiber with periodic square arrangement available in the literature. We have also compared with the tightest bounds given by Bisegna and Luciano (BL) [15] and Hashin/Shtrikman bounds (HS). We have used data reported in Pettermann and Suresh [35] which is based on the parameters measured at constant electric displacement and all EMPs are also taken from Pettermann and Suresh [35] for simulations. All the required coefficient are converted by using the relations given in Eq (9). Table 3 illustrates the comparison of the overall electromechanical constants of a piezocomposite with 60% PZT fiber V_f.

The numerical predictions of the effective coefficients using the proposed MM modeling approach showed a reasonable agreement with the other numerical models, analytical models and bounds for PCs. Note that, the results of fibers arrange in periodic square arrangements are compared. Although the results of circular fiber cross section are shown but we have also compared the square fiber cross section and similar results are obtained, not shown here. Most of the constants are identical to values reported in literature with minor differences in the effective properties of C_{44} and h_{15}. However, the discrepancies are less than 10% over the values of the analytical and numerical model presented in literature.

Table 3. Comparison of the overall constants for 60% V_f of fibers arranged in square array with circular cross section.

Material Constants	Proposed Model CF	Ber-(PBC) CF [37]	Pet-PBC CF [35]	AHM CF [37]	SCS Levin [55],	HS Bounds [35]	BL Bounds [15]

C_{11}^{D}(GPa)	25.206	25.17	25.19	24.38	21.84	24.9/28.7	25.2/25.5
C_{12}^{D}(GPa)	8.81	8.71	8.76	9.57	10.99	5.00/12.0	7.72/8.15
C_{13}^{D}(GPa)	10.87	10.82	10.84	10.84	10.51	6.12/16.5	8.89/12.3
C_{33}^{D}(GPa)	86.93	86.97	87.10	87.10	86.90	79.0/87.8	76.1/87.0
C_{44}^{D}(GPa)	6.00	6.66	6.70	7.50	6.307	6.40/7.67	6.45/6.52
C_{66}^{D}(GPa)	4.83	4.64	4.64	4.49	5.424	4.37/4.92	4.39/4.41
β_{11}(GVm/C)	6.34	6.364	6.341	5.44	6.859	2.54/6.73	6.57/6.66
β_{33}(GVm/C)	0.775	0.781	0.7808	0.779	0.779	0.74/0.95	0.73/0.84
h_{31}(GV/m)	-0.157	-0.157	-0.1568	−0.157	−0.149	−1.03/0.72	−0.33/0.024
h_{33}(GV/m)	5.005	5.039	5.0339	5.034	5.039	3.63/5.85	3.91/5.42
h_{51}(GV/m)	0.280	0.328	0.329	0.424	0.2844	−1.92/2.67	0.229/0.384

6.2 Comparison with the experimental Data

Figure of merits (FOM) are generally defined in terms of electromechanical coefficients to characterize the suitability of piezoelectric materials for ultra sound imaging, hydrophones, energy harvesting or any other commercial applications. Some of the common FOMs for ultrasonic transducer applications are the planar coupling constants $k_p = [1 - \kappa_{33}^{\varepsilon} \mathrm{C}_{33}^{D} / \kappa_{33}^{\sigma} \mathrm{C}_{33}^{E}]^{1/2}$, longitudinal velocity $V_l^D = [\mathrm{C}_{33}^{D}/\bar{\rho}]^{1/2}$ (at constant D), acoustic impedance $Z = [\bar{\rho}\mathrm{C}_{33}^{D}]^{1/2}$, thickness-mode coupling constant $k_t = [1 - \mathrm{C}_{33}^{E}/\mathrm{C}_{33}^{D}]^{1/2}$. The expression for composite density is $\bar{\rho} = \rho_m(1 - V_F) + \rho_F V_F$; where V_F, ρ_m, and ρ_F is the $\mathrm{V_f}$ of fiber, density of matrix and fiber, respectively.

The electromechanical coefficients of PZT-7A/Araldite D 1-3 piezocomposite were determined experimentally by Chan and Unsworth [14]. Table 2 shows the constituents properties used in the MM model. The results of proposed model with circular and square fiber are compared with analytical model with circular fiber (MT) and MM model with square fiber (UC), and also with experimental data.

Figure 7 shows the comparison of certain important material parameters for PZT-7A/Araldite D piezocomposite for transducer application as a function of V_f. Figures 7 (a) and (b) show the compliance $S_{11}^E + S_{12}^E$ and dielectric constant $\kappa_{33}^\sigma/\kappa_0$ with V_f of fiber while Figure 7 (c) shows the results of longitudinal velocity V_l^D with fiber V_f. The piezoelectric constant d_{33} is plotted against fiber V_f in Figure 7 (d). As discussed in

Chan and Unsworth [14], the experimentally measured value for d33 of piezofibers was ~167 pm/V, so we used this value in this study for computation of d33. The results of the MM models proposed in the current study are found in reasonable agreement with analytical models considering circular fiber (MT) and MM models with square fiber (UC).

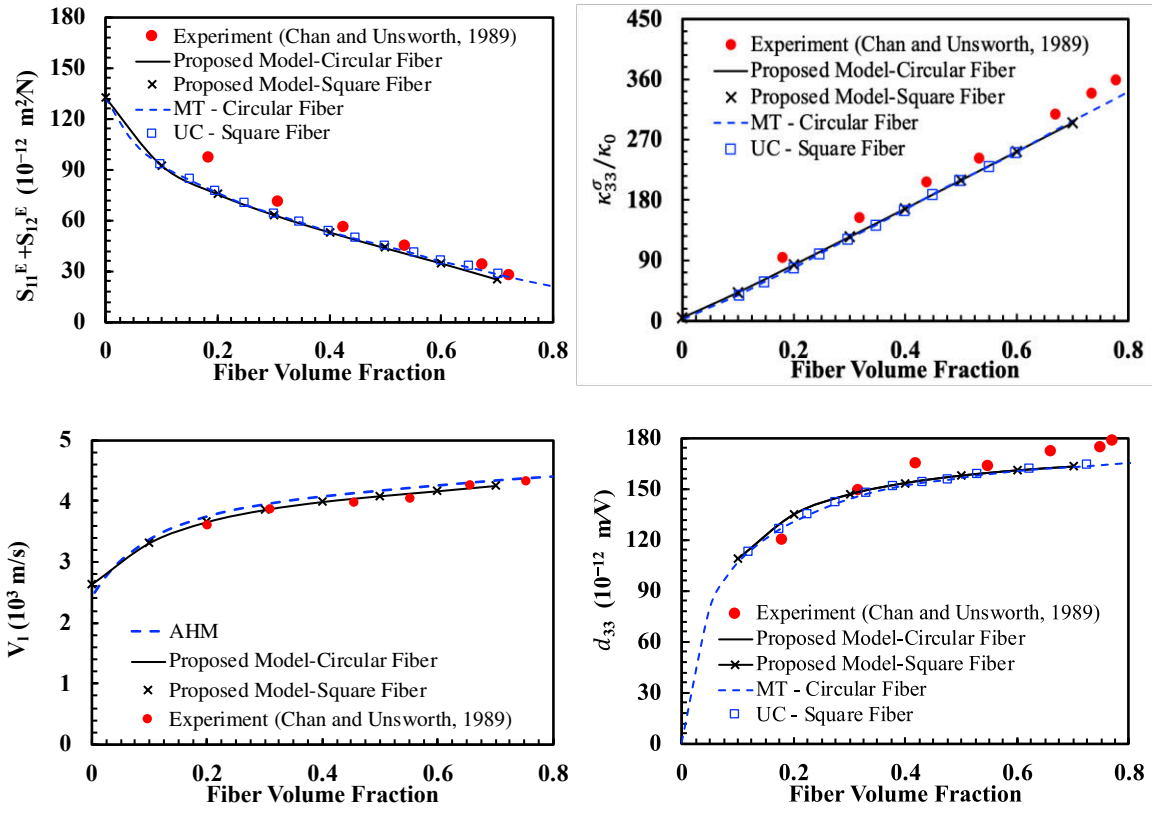

Figure 6. Comparison of material parameters for PZT-7A/Epoxy piezocomposite obtained from the MM models proposed in the current work with several other analytical models with circular fiber and MM models with square fiber; vs fiber V_f, variations of the (a) Compliance constants $S_{11}^E + S_{12}^E$, (b) relative permittivity $\kappa_{33}^\sigma/\kappa_0$, (c) longitudinal velocity V_l^D (d) piezoelectric constant d_{33}

The combination of piezoelectric fiber and matrix can yield EMPs needed for several ultrasonic transducer applications including medical imaging and hydrophones. Next we have compared the key parameters needed for the ultrasonic transducer applications that was experimentally measured by Chan and Unsworth [14]. In ultrasonic diagnostic imaging, piezoelectric materials should have high k_t for high sensitivity and low k_p help to improve image quality. The Z value should minimize reflection loses at the interface. The EMPs of the 1-3 piezocomposite can be tailored to obtain the required EMPs, such as high $k_t \sim 0.6 - 0.7$, low $Z < 7.5$ Mrayls for a comparative acoustic property, low $k_p \sim 0.3$ to improve image quality.

In Figure 8 (a) – (c), the parameters k_t, Z, and k_p are plotted against the fiber V_f, respectively. The comparisons of the current model coefficients with the experimentally measured data of Chan and Unsworth [14] produce a quite good agreement and yield similar results as obtained from the analytical solutions using AHM. The proposed MM model results display principally the identical tendency as the AHM as well as the experimental data. The PZT7A/polymer piezocomposite show $k_t \sim 0.6 - 0.7$ higher than fiber $k_t = 0.5$, low acoustic impendence $Z < 7.5$ Mrayls, $k_p \sim 0.3$ less than fiber $k_p = 0.5$. Figure 8 (d) shows the trade-off between high k_t and low Z in piezocomposite built of PZT7A piezofiber and polymeric matrix. We have observed that at low V_f i.e., less than 20% of PZT fiber a desired combination can be obtained that meets the requirement of transducer for medical applications. Results show that 1-e piezocomposite could produce a more favorable $k_t - Z$ trade-off. Castillero et al ([59] show that for the case of rectangular distribution of fibers the results of 1-3 piezocomposite can be optimized for hydrophone applications.

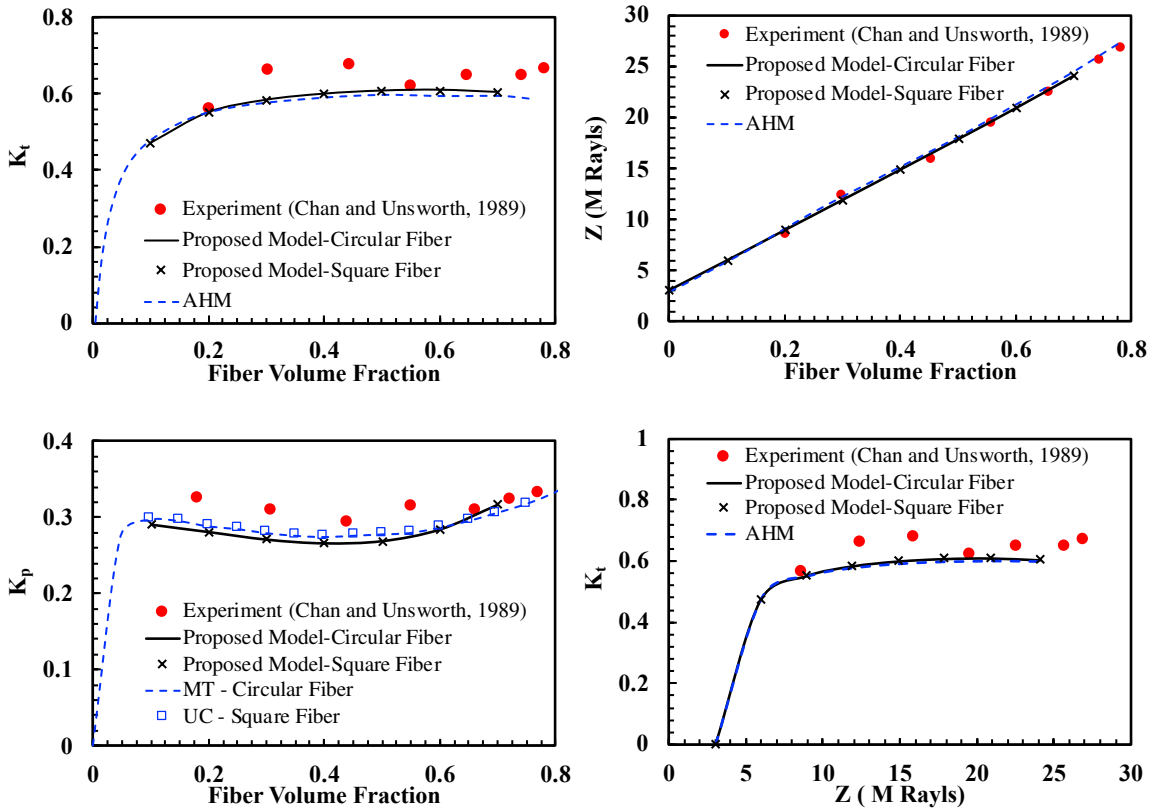

Figure 7. Comparison of material parameters for PZT-7A/Epoxy piezocomposite obtained from the MM models proposed in the current work with several other analytical models with circular fiber and MM models with square fiber; vs fiber V_f, variations of the (a) electromechanical coupling constant k_t (b) specific acoustic impedance Z (c) planar coupling constants k_p (d) k_t vs Z.

The current FE models have confirmed excellent EMPs can be achieved for the 1-3 piezocomposite. The MM model results demonstrate that the material anisotropic properties and configuration of fiber connectivity may produce wide range of architecture-dependent EMPs. The presented novel MM modeling approach have the potential to design piezocomposite with architected microstructure that could produce exceptional piezo-response.

7. Conclusions

A MM-FE homogenization method is proposed to calculate the electromechanical coefficients of the architected periodic PCs (i.e. containing architecture of fiber with circular and square cross-

section thus having 1-3 type connectivity). Using intrinsic symmetry of architecture of UC, MBCs equivalent to a PBCs are proposed. The continuity of displacements and the electric potential across UCs boundaries are ensured with that of the adjacent UCs. Results show that the 1-3 PCs exhibits a distinctive combination of responses which cannot be comprehended by bulk piezoelectric materials. Hence offers enhanced electromechanical coupling, low acoustic impedance and planar coupling coefficient indicates its suitability in transducer applications. The variation of EMPs of 1-3 PCs with fiber V_f are computed, and compared with the analytical solutions obtained using micromechanics theory, and finite-element homogenization results. A quite good agreement between the proposed modeling approach and the ones obtained using analytical is observed. However, an excellent agreement is observed with the MM results that employed PBCs. Hence, we conclude that the proposed MM modeling approach is equivalent to MM models that employed PBCs. The proposed approach is simpler and flexible for the calculation of the effective EMPs of architected PCs and their design with tunable properties while exhibiting elastic anisotropy and piezoelectric activity.

ACKNOWLEDEMENTS

This publication is based on work supported by the Khalifa University of Science and Technology under Award No. CIRA-2018-15 and Abu Dhabi Award for Research Excellence (AARE-2019) under project number 8434000349.

REFERENCES

[1] Akdogan EK, Allahverdi M, Safari A. Piezoelectric composites for sensor and actuator applications. IEEE Trans Ultrason Ferroelectr Freq Control 2005;52:746–75. https://doi.org/10.1109/TUFFC.2005.1503962.

[2] Topolov VY, Bowen CR. Electromechanical properties in composites based on ferroelectrics. Springer Science & Business Media; 2008.

[3] Swallow LM, Luo JK, Siores E, Patel I, Dodds D. A piezoelectric fibre composite based energy harvesting device for potential wearable applications. Smart Mater Struct 2008;17:025017. https://doi.org/10.1088/0964-1726/17/2/025017.

[4] Skinner DP, Newnham RE, Cross LE. Flexible composite transducers. Mater Res Bull 1978;13:599–607.
[5] Bent AA, Hagood NW. Piezoelectric Fiber Composites with Interdigitated Electrodes. J Intell Mater Syst Struct 1997;8:903–19. https://doi.org/10.1177/1045389X9700801101.
[6] Wadley HN. Multifunctional periodic cellular metals. Philos Trans R Soc Lond Math Phys Eng Sci 2006;364:31–68.
[7] Sun P, Wang G, Wu D, Zhu B, Hu C, Liu C, et al. High Frequency PMN-PT 1-3 Composite Transducer for Ultrasonic Imaging Application. Ferroelectrics 2010;408:120–8. https://doi.org/10.1080/00150193.2010.485546.
[8] Newnham RE, Skinner DP, Cross LE. Connectivity and piezoelectric-pyroelectric composites. Mater Res Bull 1978;13:525–36. https://doi.org/10.1016/0025-5408(78)90161-7.
[9] Reed DM, Srinivasan TT, Xu QC, Newnham RR. Effect of particle size on the dielectric and piezoelectric properties of PbTiO/sub 3/-polymer composites. Appl. Ferroelectr. 1990 IEEE 7th Int. Symp. On, IEEE; 1990, p. 324–327.
[10] Wang DY, Li K, Chan HLW. Lead-free BNBT-6 piezoelectric ceramic fibre/epoxy 1-3 composites for ultrasonic transducer applications. Appl Phys A 2005;80:1531–4. https://doi.org/10.1007/s00339-003-2390-3.
[11] Chen Y-C, Wu S. Piezoelectric composites with 3-3 connectivity by injecting polymer for hydrostatic sensors. Ceram Int 2004;30:69–74.
[12] Haun MJ, Newnham RE. An experimental and theoretical study of 1–3 AND 1-3-0 piezoelectric PZT-Polymer composites for hydrophone applications. Ferroelectrics 1986;68:123–139.
[13] Smith WA, Auld BA. Modeling 1-3 composite piezoelectrics: thickness-mode oscillations. Ultrason Ferroelectr Freq Control IEEE Trans On 1991;38:40–47.
[14] Chan HLW, Unsworth J. Simple model for piezoelectric ceramic/polymer 1-3 composites used in ultrasonic transducer applications. Ultrason Ferroelectr Freq Control IEEE Trans On 1989;36:434–441.
[15] Bisegna P, Luciano R. On methods for bounding the overall properties of periodic piezoelectric fibrous composites. J Mech Phys Solids 1997;45:1329–56. https://doi.org/10.1016/S0022-5096(96)00116-0.
[16] Bisegna P, Luciano R. Variational bounds for the overall properties of piezoelectric composites. J Mech Phys Solids 1996;44:583–602. https://doi.org/10.1016/0022-5096(95)00084-4.
[17] Benveniste Y. Exact results in the micromechanics of fibrous piezoelectric composites exhibiting pyroelectricity. Proc. R. Soc. Lond. Math. Phys. Eng. Sci., vol. 441, The Royal Society; 1993, p. 59–81.
[18] Chen T. Piezoelectric properties of multiphase fibrous composites: Some theoretical results. J Mech Phys Solids 1993;41:1781–94. https://doi.org/10.1016/0022-5096(93)90031-A.
[19] Dunn ML. Electroelastic Green's functions for transversely isotropic piezoelectric media and their application to the solution of inclusion and inhomogeneity problems. Int J Eng Sci 1994;32:119–31. https://doi.org/10.1016/0020-7225(94)90154-6.
[20] Biao W. Three-dimensional analysis of an ellipsoidal inclusion in a piezoelectric material. Int J Solids Struct 1992;29:293–308. https://doi.org/10.1016/0020-7683(92)90201-4.

[21] Jiang B, Fang D-N, Hwang K-C. A unified model for piezocomposites with non-piezoelectric matrix and piezoelectric ellipsoidal inclusions. Int J Solids Struct 1999;36:2707–33. https://doi.org/10.1016/S0020-7683(98)00125-5.
[22] Mori T, Tanaka K. Average stress in matrix and average elastic energy of materials with misfitting inclusions. Acta Metall 1973. https://doi.org/10.1016/0001-6160(73)90064-3.
[23] Dunn ML, Taya M. Micromechanics predictions of the effective electroelastic moduli of piezoelectric composites. Int J Solids Struct 1993;30:161–175.
[24] Nan C-W. Effective-medium theory of piezoelectric composites. J Appl Phys 1994;76:1155–1163.
[25] Lin C-H, Muliana A. Micromechanics models for the effective nonlinear electro-mechanical responses of piezoelectric composites. Acta Mech 2013;224:1471–92. https://doi.org/10.1007/s00707-013-0823-4.
[26] Bravo-Castillero J, Guinovart-Díaz R, Sabina FJ, Rodríguez-Ramos R. Closed-form expressions for the effective coefficients of a fiber-reinforced composite with transversely isotropic constituents – II. Piezoelectric and square symmetry. Mech Mater 2001;33:237–48. https://doi.org/10.1016/S0167-6636(00)00060-0.
[27] Rodríguez-Ramos R, Sabina FJ, Guinovart-Díaz R, Bravo-Castillero J. Closed-form expressions for the effective coefficients of a fiber-reinforced composite with transversely isotropic constituents – I. Elastic and square symmetry. Mech Mater 2001;33:223–35. https://doi.org/10.1016/S0167-6636(00)00059-4.
[28] Guinovart-Díaz R, Bravo-Castillero J, Rodríguez-Ramos R, Sabina FJ. Closed-form expressions for the effective coefficients of fibre-reinforced composite with transversely isotropic constituents. I: Elastic and hexagonal symmetry. J Mech Phys Solids 2001;49:1445–62. https://doi.org/10.1016/S0022-5096(01)00005-9.
[29] Sabina FJ, Rodríguez-Ramos R, Bravo-Castillero J, Guinovart-Díaz R. Closed-form expressions for the effective coefficients of a fibre-reinforced composite with transversely isotropic constituents. II: Piezoelectric and hexagonal symmetry. J Mech Phys Solids 2001;49:1463–79. https://doi.org/10.1016/S0022-5096(01)00006-0.
[30] Aboudi J. Micromechanical prediction of the effective coefficients of thermo-piezoelectric multiphase composites 1998.
[31] Gohari S, Sharifi S, Vrcelj Z. New explicit solution for static shape control of smart laminated cantilever piezo-composite-hybrid plates/beams under thermo-electro-mechanical loads using piezoelectric actuators. Compos Struct 2016;145:89–112. https://doi.org/10.1016/j.compstruct.2016.02.047.
[32] Gohari S, Sharifi S, Vrcelj Z. A novel explicit solution for twisting control of smart laminated cantilever composite plates/beams using inclined piezoelectric actuators. Compos Struct 2017;161:477–504. https://doi.org/10.1016/j.compstruct.2016.11.063.
[33] Gohari S, Sharifi S, Abadi R, Izadifar M, Burvill C, Vrcelj Z. A quadratic piezoelectric multi-layer shell element for FE analysis of smart laminated composite plates induced by MFC actuators. Smart Mater Struct 2018;27:095004. https://doi.org/10.1088/1361-665X/aacc95.
[34] Tu J, Zhang J, Li Z, Gao K, Liu M. Research on actuation performance of macro fiber composites based on third order shear deformation theory. Smart Mater Struct 2019;29:015038. https://doi.org/10.1088/1361-665X/ab47d5.
[35] Pettermann HE, Suresh S. A comprehensive unit cell model: a study of coupled effects in piezoelectric 1–3 composites. Int J Solids Struct 2000;37:5447–5464.

[36] Odegard GM. Constitutive modeling of piezoelectric polymer composites. Acta Mater 2004;52:5315–5330.
[37] Berger H, Kari S, Gabbert U, Rodriguez-Ramos R, Bravo-Castillero J, Guinovart-Diaz R, et al. Unit cell models of piezoelectric fiber composites for numerical and analytical calculation of effective properties. Smart Mater Struct 2006;15:451.
[38] Wickramasinghe VK, Hagood NW. Material characterization of active fiber composites for integral twist-actuated rotor blade application. Smart Mater Struct 2004;13:1155.
[39] Ramesh R, Prasad CD, Kumar TKV, Gavane LA, Vishnubhatla RMR. Experimental and finite element modelling studies on single-layer and multi-layer 1–3 piezocomposite transducers. Ultrasonics 2006;44:341–9. https://doi.org/10.1016/j.ultras.2006.02.001.
[40] Kar-Gupta R, Venkatesh TA. Electromechanical response of 1–3 piezoelectric composites: A numerical model to assess the effects of fiber distribution. Acta Mater 2007;55:1275–1292.
[41] Khan KA, Al-Mansoor S, Khan SZ, Khan MA. Piezoelectric Metamaterial with Negative and Zero Poisson's Ratios. J Eng Mech 2019;145:04019101. https://doi.org/10.1061/(ASCE)EM.1943-7889.0001674.
[42] Kamran A. Khan, Hamad K. Alarafati, Muhammad Ali Khan. Micromechanical modeling of architected piezoelectric foam with simplified boundary conditions for hydrophone applications. J Intell Mater Syst Struct 2020;1:1–15.
[43] Tajeddini V, Lin C-H, Muliana A, Lévesque M. Average electro-mechanical properties and responses of active composites. Comput Mater Sci 2014;82:405–414.
[44] Berger H, Kari S, Gabbert U, Rodriguez-Ramos R, Bravo-Castillero J, Guinovart-Diaz R. Calculation of effective coefficients for piezoelectric fiber composites based on a general numerical homogenization technique. Compos Struct 2005;71:397–400. https://doi.org/10.1016/j.compstruct.2005.09.038.
[45] Yang J. An Introduction to the Theory of Piezoelectricity. Springer Science & Business Media; 2006.
[46] Khan KA, Abu Al-Rub RK. Time dependent response of architectured Neovius foams. Int J Mech Sci 2017;126:106–19. https://doi.org/10.1016/j.ijmecsci.2017.03.017.
[47] Kanit T, Forest S, Galliet I, Mounoury V, Jeulin D. Determination of the size of the representative volume element for random composites: statistical and numerical approach. Int J Solids Struct 2003;40:3647–3679.
[48] Khan KA, Muliana AH. A multi-scale model for coupled heat conduction and deformations of viscoelastic functionally graded materials. Compos Part B Eng 2009;40:511–21. https://doi.org/10.1016/j.compositesb.2009.02.003.
[49] Choudhry RS, Khan KA, Khan SZ, Khan MA, Hassan A. Micromechanical modeling of 8-harness satin weave glass fiber-reinforced composites. J Compos Mater 2016:0021998316649782. https://doi.org/10.1177/0021998316649782.
[50] Jiang M, Jasiuk I, Ostoja-Starzewski M. Apparent thermal conductivity of periodic two-dimensional composites. Comput Mater Sci 2002;25:329–338.
[51] Xia Z, Zhang Y, Ellyin F. A unified periodical boundary conditions for representative volume elements of composites and applications. Int J Solids Struct 2003;40:1907–21. https://doi.org/10.1016/S0020-7683(03)00024-6.
[52] Li S. Boundary conditions for unit cells from periodic microstructures and their implications. Compos Sci Technol 2008;68:1962–1974.

[53] Khan KA, Khan MA. 3-3 piezoelectric metamaterial with negative and zero Poisson's ratio for hydrophones applications. Mater Res Bull 2019;112:194–204. https://doi.org/10.1016/j.materresbull.2018.12.016.
[54] Dunn ML, Taya M. Electromechanical Properties of Porous Piezoelectric Ceramics. J Am Ceram Soc 1993;76:1697–706. https://doi.org/10.1111/j.1151-2916.1993.tb06637.x.
[55] Levin VM, Sabina FJ, Bravo-Castillero J, Guinovart-Díaz R, Rodríguez-Ramos R, Valdiviezo-Mijangos OC. Analysis of effective properties of electroelastic composites using the self-consistent and asymptotic homogenization methods. Int J Eng Sci 2008;46:818–34. https://doi.org/10.1016/j.ijengsci.2008.01.017.
[56] Guinovart-Dıaz R, Bravo-Castillero J, Rodrıguez-Ramos R, Sabina FJ, Martınez-Rosado R. Overall properties of piezocomposite materials 1–3. Mater Lett 2001;48:93–98.
[57] Berger H, Kari S, Gabbert U, Rodriguez-Ramos R, Guinovart R, Otero JA, et al. An analytical and numerical approach for calculating effective material coefficients of piezoelectric fiber composites. Int J Solids Struct 2005;42:5692–714. https://doi.org/10.1016/j.ijsolstr.2005.03.016.
[58] Hashin Z, Shtrikman S. On some variational principles in anisotropic and nonhomogeneous elasticity. J Mech Phys Solids 1962;10:335–42. https://doi.org/10.1016/0022-5096(62)90004-2.
[59] Castillero JB, Diaz RG, Hernandez JAO, Ramos RR. Electromechanical properties of continuous fibre-reinforced piezoelectric composites. Mech Compos Mater 1997;33:475–82. https://doi.org/10.1007/BF02256903.